

Micromechanical modeling of the multiphysical behavior of smart materials using the variational asymptotic method

This article has been downloaded from IOPscience. Please scroll down to see the full text article.

2009 Smart Mater. Struct. 18 125026

(<http://iopscience.iop.org/0964-1726/18/12/125026>)

View [the table of contents for this issue](#), or go to the [journal homepage](#) for more

Download details:

IP Address: 130.18.101.166

The article was downloaded on 26/05/2010 at 14:38

Please note that [terms and conditions apply](#).

Micromechanical modeling of the multiphysical behavior of smart materials using the variational asymptotic method*

Tian Tang¹ and Wenbin Yu

Department of Mechanical and Aerospace Engineering, Logan, UT 84322-4130, USA

Received 24 August 2009, in final form 15 October 2009

Published 10 November 2009

Online at stacks.iop.org/SMS/18/125026

Abstract

A multiphysics micromechanics model is developed to predict the effective properties as well as the local fields of periodic smart materials responsive to fully coupled electric, magnetic, thermal and mechanical fields. This work is based on the framework of the variational asymptotic method for unit cell homogenization (VAMUCH), a recently developed micromechanics modeling scheme. To treat the general microstructure of smart materials, we implemented this model using the finite element technique. Several examples of smart materials are used to demonstrate the application of the proposed model for prediction of multiphysical behavior.

(Some figures in this article are in colour only in the electronic version)

1. Introduction

Smart materials are responsive to multiple fields, such as electric, magnetic or thermal fields, in addition to the traditional mechanical field. Multiphysical behavior of such materials will be coupled and analysis tools with predictive capabilities are essential for effective design and analysis of such materials. In addition to the complexity due to the interplay of multiple fields, smart materials are also engineered with more than one single constituent for the desirable performance needed for real applications. Furthermore, such heterogeneous smart materials might exhibit new properties not existing in any of the constituents due to the coupling of different fields. For example, the most interesting behavior of smart composites consisting of piezoelectric and piezomagnetic constituents is that the magneto-electric effect, which is only present in composites but absent in constituent phases, is created by the interaction between the constituent phases, a result of the so-called product property [1]. The mechanical constitutive response of the active materials can be coupled with the non-mechanical effects [2]. For example, a piezoelectric material under a temperature field

can exhibit piezoelectric, along with pyroelectric, effects. It has been experimentally observed that an interphase region exists between an inclusion and the surrounding matrix. This interphase region is of the same length scale as the particulate inclusion and could play an important role in the macroscopic properties of the composites [3]. The importance of this interphase in the product property is also investigated analytically using homogenization techniques [4, 5].

Generally speaking, smart materials could have fully coupled electro-magneto-thermo-elastic behavior which exhibits both piezoelectric and piezomagnetic coupling effects as well as pyroelectric, pyromagnetic and electromagnetic effects. For linear behavior among all these fields, the constitutive equations can be expressed as

$$\begin{aligned}\sigma_{ij} &= C_{ijkl}\varepsilon_{kl} - e_{kij}E_k - q_{kij}H_k + \Lambda_{ij}\theta \\ D_i &= e_{ikl}\varepsilon_{kl} + k_{ik}E_k + a_{ik}H_k + p_i\theta \\ B_i &= q_{ikl}\varepsilon_{kl} + a_{ik}E_k + \mu_{ik}H_k + m_i\theta\end{aligned}\quad (1)$$

where C_{ijkl} , e_{kij} , q_{kij} and Λ_{ij} are the elastic, piezoelectric, piezomagnetic and thermal stress tensors, respectively (note that $\Lambda_{ij} = -C_{ijkl}\alpha_{kl}$ with α_{kl} as the thermal expansion strain tensor); σ_{ij} and ε_{ij} are the stress tensor and strain tensor, respectively; k_{ik} , a_{ik} and μ_{ik} are the dielectric, magneto-electric and magnetic permeability tensors, respectively; p_i and m_i are the pyroelectric and pyromagnetic vectors; D_i , E_k ,

* A preliminary version of this paper was presented at the 2008 ASME Conference on Smart Materials, Adaptive Structures and Intelligent Systems, Ellicott City, MD, USA.

¹ Present address: Center of Advanced Vehicular Systems, Mississippi State University, MS 39762, USA.

B_i and H_i are the electric displacement, electric field, magnetic induction and magnetic field vectors. θ denotes the difference between the actual temperature and the reference temperature. Here and throughout this paper, Latin indices assume 1, 2 and 3 and repeated indices are summed over their range except where explicitly indicated.

Li and Dunn [6] employed the Mori–Tanaka method [7] for predicting the average fields and effective moduli of fully coupled magneto-electro-elastic composites where the closed-form expressions are obtained for effective magneto-electro-elastic properties of circular cylinder fibrous and laminated two-phase composites. Aboudi [8] developed a micromechanics method for the prediction of the effective properties of magneto-electro-thermo-elastic composites using the framework of the high-fidelity generalized method of cells. The predictions of this model agree well with those of the Mori–Tanaka model. Lee *et al* [9] developed a finite-element-analysis-based micromechanics approach through averaging of the representative volume element (RVE) to determine the effective dielectric, magnetic, mechanical and coupled-field properties of this composite as functions of the phase volume fractions, the fiber arrangements in RVE and the fiber material properties with special emphasis on the poling directions of the piezoelectric and piezomagnetic fibers. The authors recently developed a micromechanics approach for the prediction of the effective properties and local fields of heterogeneous electro-magneto-elastic materials [10]. The work is based on the framework of the variational asymptotic method for unit cell homogenization (VAMUCH) [11–14], in which the unit cell (UC) is defined as an RVE with the smallest possible size. VAMUCH is an application of the variational asymptotic method (VAM) [15] to micromechanics. It carries out an asymptotic analysis of the governing functional to find the corresponding asymptotic expansion of the field variables, which is different from the well-known two-scale asymptotic homogenization theory (AHM) [16–18]. In AHM, also called mathematical homogenization theories (MHT), the solution is sought in the form of multiscale asymptotic series which can be obtained through a formal asymptotic analysis of the governing differential equations along with assumed periodic boundary conditions for the *a priori* unknown functions in fast variables, while in VAMUCH, both the multiscale asymptotic series and the periodic boundary conditions are derived from the asymptotic analysis of the governing functional.

In this paper, we are going to extend VAMUCH for smart heterogeneous composites to capture the fully coupled multiphysical behavior including electric, magnetic, thermal and elastic behavior and their interactions. The resulting theory and companion code will be able to predict effective multiphysical properties (including the effective elastic, piezoelectric, piezomagnetic and magneto-electric coupling coefficients as well as the thermal stress coefficients, pyroelectric constants, pyromagnetic constants and specific heats) and calculate the local multiphysical field distribution within the microstructure. This work is build upon the variational asymptotic method [19] along with two essential assumptions associated with the micromechanics concept for heterogeneous materials:

- **Assumption 1.** The exact solutions of the field variables have volume averages over UC. For example, if u_i , ϕ^e and ϕ^m are the exact displacements, electric potential and magnetic potential within the UC occupying a volume Ω , respectively, there exist v_i , ψ^e and ψ^m such that

$$\begin{aligned} v_i &= \frac{1}{\Omega} \int_{\Omega} u_i \, d\Omega \equiv \langle u_i \rangle \\ \psi^e &= \frac{1}{\Omega} \int_{\Omega} \phi^e \, d\Omega \equiv \langle \phi^e \rangle \\ \psi^m &= \frac{1}{\Omega} \int_{\Omega} \phi^m \, d\Omega \equiv \langle \phi^m \rangle. \end{aligned} \quad (2)$$

- **Assumption 2.** The effective material properties obtained from the micromechanical analysis of the UC are independent of the geometry, the boundary conditions and loading conditions of the macroscopic structure, which means that effective properties are assumed to be the intrinsic properties of the material when viewed macroscopically.

Note that these assumptions are not restrictive. The mathematical meaning of the first assumption is that the exact solutions of the field variables are integrable over the domain of the UC, which is true almost all the time and the very basic requirement for us to perform the homogenization. The second assumption implies that we can neglect the size effects and loading effects of the material properties in the macroscopic analysis, which is an assumption often made in the conventional continuum mechanics necessary for the definition of material properties. Of course, the micromechanical analysis of the UC is only needed and appropriate if $h/l \ll 1$ with h as the characteristic size of the UC and l as the characteristic length scale of the macroscopic behavior of the heterogeneous material. Other assumptions common in the literature such as a particular geometry shape and arrangement of the constituents, specific boundary conditions applied to the UC and prescribed relations between local fields and global fields are not needed for this study.

2. Theoretical formulation

Three coordinates are used in our formulation including two Cartesian coordinates $\mathbf{x} = (x_1, x_2, x_3)$ and $\mathbf{y} = (y_1, y_2, y_3)$, and an integer-valued coordinate $\mathbf{n} = (n_1, n_2, n_3)$; see figure 1. We use x_i as the global coordinates to describe the macroscopic structure and y_i parallel to x_i as the local coordinates to describe the UC. We choose the origin of the local coordinates y_i to be the geometric center of the UC. To uniquely locate a UC in the heterogeneous material we also introduce integer coordinates n_i . The integer coordinates are related to the global coordinates in such a way that $n_i = x_i/d_i$, with d_i denoting the edge lengths of the UC (no summation over i). It is emphasized that, although only a two-dimensional (2D) UC is sketched in figure 1, the present theory has no such limitations and is also capable of handling other microstructures including one-dimensional (1D) and three-dimensional (3D) UCs.

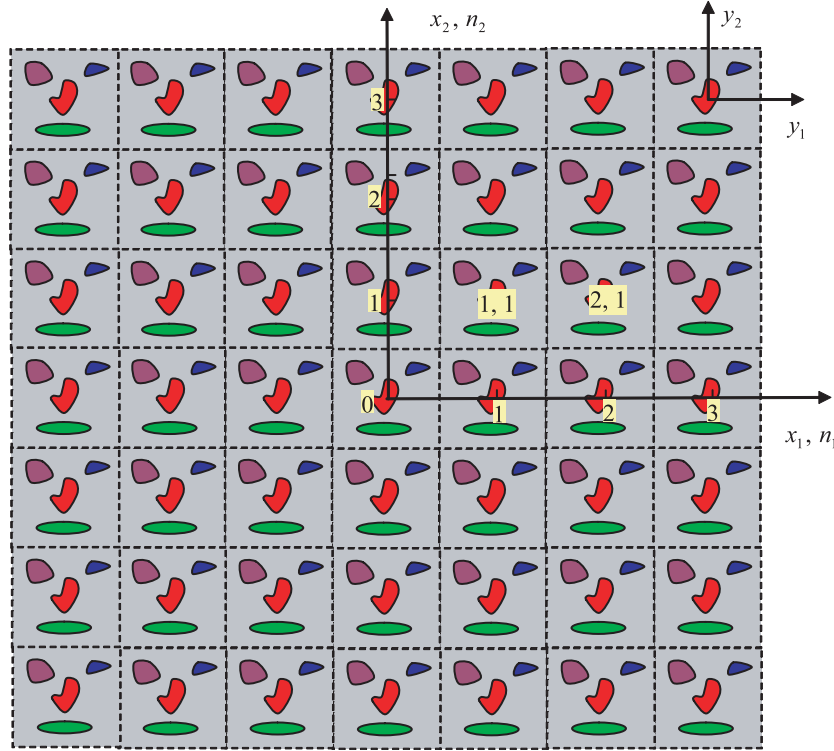


Figure 1. Coordinate systems for heterogeneous materials (only 2D UC is drawn for clarity).

The VAMUCH formulation starts from a variational statement of the continuum mechanics description of the multiphysical behavior of smart materials. For this purpose, we need to express the thermodynamic potential corresponding to the constitutive equations in (1) as

$$U = \frac{1}{2} \epsilon^T L \epsilon + \epsilon^T \eta \theta + \frac{1}{2} c_v \frac{\theta^2}{T_0} \quad (3)$$

where

$$\epsilon = [\epsilon_{11} \quad 2\epsilon_{12} \quad \epsilon_{22} \quad 2\epsilon_{13} \quad 2\epsilon_{23} \quad \epsilon_{33} \\ E_1 \quad E_2 \quad E_3 \quad H_1 \quad H_2 \quad H_3]^T \quad (4)$$

is a multiphysical field vector containing the 3D strain field ϵ_{ij} , the 3D electric field E_i and the 3D magnetic field H_i , which are defined for a linear theory as

$$\epsilon_{ij}(\mathbf{n}; \mathbf{y}) = \frac{1}{2} \left[\frac{\partial u_i(\mathbf{n}; \mathbf{y})}{\partial y_j} + \frac{\partial u_j(\mathbf{n}; \mathbf{y})}{\partial y_i} \right] \\ E_i(\mathbf{n}; \mathbf{y}) = - \frac{\partial \phi^e(\mathbf{n}; \mathbf{y})}{\partial y_i} \\ H_i(\mathbf{n}; \mathbf{y}) = - \frac{\partial \phi^m(\mathbf{n}; \mathbf{y})}{\partial y_i} \quad (5)$$

and L is a 12×12 multiphysics matrix containing all the necessary material constants for characterizing completely coupled electro-magneto-elastic materials such that

$$L = \begin{bmatrix} C & -e & -q \\ -e^T & -k & -a \\ -q^T & -a^T & -\mu \end{bmatrix} \quad (6)$$

where C is a 6×6 submatrix for elastic constants, e is a 6×3 submatrix for piezoelectric coefficients, q is a 6×3 submatrix for piezomagnetic coefficients, k is a 3×3 submatrix for dielectric coefficients, a is a 3×3 submatrix for electromagnetic coefficients and μ is a 3×3 submatrix for magnetic permeability. Other terms in equation (3) include η , which is a 12×1 matrix containing the second-order thermal stress tensor Λ_{ij} , the vector of pyroelectric p_i and the vector of pyromagnetic m_i expressed as

$$\eta = [\Lambda_{11} \quad \Lambda_{12} \quad \Lambda_{22} \quad \Lambda_{13} \quad \Lambda_{23} \quad \Lambda_{33} \\ p_1 \quad p_2 \quad p_3 \quad m_1 \quad m_2 \quad m_3]^T.$$

The coefficient in front of the last term c_v is the specific heat per unit volume at constant volume, while T_0 is the reference temperature at which the constituent material is stress-free.

The second assumption implies that we could obtain the same effective material properties from an imaginary unbounded and unloaded smart material with the same microstructure as the loaded and bounded one. Hence we could derive the micromechanical analysis from a smart material which could completely occupy the 3D space \mathcal{R} and is composed of infinitely many UCs. The total thermodynamic potential of this imaginary material is equal to the summation of the thermodynamic potential stored in all the UCs, which is

$$\Pi = \sum_{n=-\infty}^{\infty} \int_{\Omega} U \, d\Omega. \quad (7)$$

In view of the fact that the infinitely many UCs form a continuous heterogeneous material, we need to enforce the continuity of the displacement field u_i , the electric potential

field ϕ^e and the magnetic potential ϕ^m on the interface between adjacent UCs, which are

$$\begin{aligned}
& u_i(n_1, n_2, n_3; d_1/2, y_2, y_3) \\
&= u_i(n_1 + 1, n_2, n_3; -d_1/2, y_2, y_3) \\
& u_i(n_1, n_2, n_3; y_1, d_2/2, y_3) \\
&= u_i(n_1, n_2 + 1, n_3; y_1, -d_2/2, y_3) \\
& u_i(n_1, n_2, n_3; y_1, y_2, d_3/2) \\
&= u_i(n_1, n_2, n_3 + 1; y_1, y_2, -d_3/2) \\
& \phi^e(n_1, n_2, n_3; d_1/2, y_2, y_3) \\
&= \phi^e(n_1 + 1, n_2, n_3; -d_1/2, y_2, y_3) \\
& \phi^e(n_1, n_2, n_3; y_1, d_2/2, y_3) \\
&= \phi^e(n_1, n_2 + 1, n_3; y_1, -d_2/2, y_3) \\
& \phi^e(n_1, n_2, n_3; y_1, y_2, d_3/2) \\
&= \phi^e(n_1, n_2, n_3 + 1; y_1, y_2, -d_3/2) \\
& \phi^m(n_1, n_2, n_3; d_1/2, y_2, y_3) \\
&= \phi^m(n_1 + 1, n_2, n_3; -d_1/2, y_2, y_3) \\
& \phi^m(n_1, n_2, n_3; y_1, d_2/2, y_3) \\
&= \phi^m(n_1, n_2 + 1, n_3; y_1, -d_2/2, y_3) \\
& \phi^m(n_1, n_2, n_3; y_1, y_2, d_3/2) \\
&= \phi^m(n_1, n_2, n_3 + 1; y_1, y_2, -d_3/2).
\end{aligned}$$

The smart heterogeneous materials considered here are subjected to a uniform temperature deviation θ . Therefore, the continuity condition for the temperature field between adjacent UCs is automatically satisfied. The exact solution of the present problem will minimize the summation of the thermodynamic potential in equation (7) under the conditions in equations (2) and (8). To avoid the difficulty associated with discrete integer arguments, we can reformulate the problem, including (5), (7) and (8) in terms of continuous functions using the idea of a quasicontinuum [20]. The corresponding formulae are listed below:

$$\Pi = \int_{\mathcal{R}} \left\langle \frac{1}{2} \epsilon^T L \epsilon + \epsilon^T \eta \theta + \frac{1}{2} c_v \frac{\theta^2}{T_0} \right\rangle d\mathcal{R} \quad (9)$$

$$\varepsilon_{ij}(\mathbf{x}; \mathbf{y}) = \frac{1}{2} \left[\frac{\partial u_i(\mathbf{x}; \mathbf{y})}{\partial y_j} + \frac{\partial u_j(\mathbf{x}; \mathbf{y})}{\partial y_i} \right] \equiv u_{(ij)} \quad (10)$$

$$E_i(\mathbf{x}; \mathbf{y}) = - \frac{\partial \phi^e(\mathbf{x}; \mathbf{y})}{\partial y_i} \quad (11)$$

$$H_i(\mathbf{x}; \mathbf{y}) = - \frac{\partial \phi^m(\mathbf{x}; \mathbf{y})}{\partial y_i} \quad (12)$$

and

$$\begin{aligned}
& u_i(x_1, x_2, x_3; d_1/2, y_2, y_3) \\
&= u_i(x_1 + d_1, x_2, x_3; -d_1/2, y_2, y_3) \\
& u_i(x_1, x_2, x_3; y_1, d_2/2, y_3) \\
&= u_i(x_1, x_2 + d_2, x_3; y_1, -d_2/2, y_3) \\
& u_i(x_1, x_2, x_3; y_1, y_2, d_3/2) \\
&= u_i(x_1, x_2, x_3 + d_3; y_1, y_2, -d_3/2) \\
& \phi^e(x_1, x_2, x_3; d_1/2, y_2, y_3) \\
&= \phi^e(x_1 + d_1, x_2, x_3; -d_1/2, y_2, y_3) \\
& \phi^e(x_1, x_2, x_3; y_1, d_2/2, y_3) \\
&= \phi^e(x_1, x_2 + d_2, x_3; y_1, -d_2/2, y_3) \\
& \phi^e(x_1, x_2, x_3; y_1, y_2, d_3/2) \\
&= \phi^e(x_1, x_2, x_3 + d_3; y_1, y_2, -d_3/2) \\
& \phi^m(x_1, x_2, x_3; d_1/2, y_2, y_3) \\
&= \phi^m(x_1 + d_1, x_2, x_3; -d_1/2, y_2, y_3) \\
& \phi^m(x_1, x_2, x_3; y_1, d_2/2, y_3) \\
&= \phi^m(x_1, x_2 + d_2, x_3; y_1, -d_2/2, y_3) \\
& \phi^m(x_1, x_2, x_3; y_1, y_2, d_3/2) \\
&= \phi^m(x_1, x_2, x_3 + d_3; y_1, y_2, -d_3/2).
\end{aligned} \quad (13)$$

Introducing Lagrange multipliers, we can pose the variational statement of the micromechanical analysis of UCs as a stationary value problem of the following functional:

$$\begin{aligned}
J = \int_{\mathcal{R}} \left\{ \frac{1}{2} \epsilon^T L \epsilon + \epsilon^T \eta \theta + \frac{1}{2} c_v \frac{\theta^2}{T_0} \right\} + \lambda_i (\langle u_i \rangle - v_i) \\
+ \lambda^e (\langle \phi \rangle^e - \psi^e) + \lambda^m (\langle \phi \rangle^m - \psi^m) \\
+ \int_{S_1} \gamma_{i1} [u_i(x_j; d_1/2, y_2, y_3) \\
- u_i(x_j + \delta_{j1} d_1; -d_1/2, y_2, y_3)] dS_1 \\
+ \int_{S_2} \gamma_{i2} [u_i(x_j; y_1, d_2/2, y_3) \\
- u_i(x_j + \delta_{j2} d_2; y_1, -d_2/2, y_3)] dS_2 \\
+ \int_{S_3} \gamma_{i3} [u_i(x_j; y_1, y_2, d_3/2) \\
- u_i(x_j + \delta_{j3} d_3; y_1, y_2, -d_3/2)] dS_3 \\
+ \int_{S_1} \alpha_1 [\phi^e(x_j; d_1/2, y_2, y_3) \\
- \phi^e(x_j + \delta_{j1} d_1; -d_1/2, y_2, y_3)] dS_1 \\
+ \int_{S_2} \alpha_2 [\phi^e(x_j; y_1, d_2/2, y_3) \\
- \phi^e(x_j + \delta_{j2} d_2; y_1, -d_2/2, y_3)] dS_2 \\
+ \int_{S_3} \alpha_3 [\phi^e(x_j; y_1, y_2, d_3/2) \\
- \phi^e(x_j + \delta_{j3} d_3; y_1, y_2, -d_3/2)] dS_3 \\
+ \int_{S_1} \beta_1 [\phi^m(x_j; d_1/2, y_2, y_3)
\end{aligned}$$

$$\begin{aligned}
 & -\phi^m(x_j + \delta_{j1}d_1; -d_1/2, y_2, y_3)] dS_1 \\
 & + \int_{S_2} \beta_2[\phi^m(x_j; y_1, d_2/2, y_3) \\
 & - \phi^m(x_j + \delta_{j2}d_2; y_1, -d_2/2, y_3)] dS_2 \\
 & + \int_{S_3} \beta_3[\phi^m(x_j; y_1, y_2, d_3/2) \\
 & - \phi^m(x_j + \delta_{j3}d_3; y_1, y_2, -d_3/2)] dS_3 \Big\} d\mathcal{R} \quad (14)
 \end{aligned}$$

where $\lambda_i, \lambda^e, \lambda^m, \gamma_{ij}, \alpha_i$ and β_i are Lagrange multipliers introduced to enforce the constraints in equations (2) and (13), S_i is the boundary surface normal to the coordinate y_i , x_j represents the triplet of x_1, x_2, x_3 and δ_{ij} is the Kronecker delta.

The main objective of micromechanics is to find the microscopic field variables u_i, ϕ^e and ϕ^m in terms of the macroscopic field variables v_i, ψ^e and ψ^m , which is a very difficult problem because we have to solve this stationary problem for each point in the global system x_i as in equation (14). It will be desirable if we can formulate the variational statement posed over a single UC only. In view of equations (2), it is natural to express the microscopic field variables in terms of the macroscopic field variables plus the differences, such that

$$\begin{aligned}
 u_i(\mathbf{x}; \mathbf{y}) &= v_i(\mathbf{x}) + w_i(\mathbf{x}; \mathbf{y}) \\
 \phi^e(\mathbf{x}; \mathbf{y}) &= \psi^e(\mathbf{x}) + w^e(\mathbf{x}; \mathbf{y}) \\
 \phi^m(\mathbf{x}; \mathbf{y}) &= \psi^m(\mathbf{x}) + w^m(\mathbf{x}; \mathbf{y})
 \end{aligned} \quad (15)$$

with

$$\langle w_i \rangle = 0 \quad \langle w^e \rangle = 0 \quad \langle w^m \rangle = 0 \quad (16)$$

according to equations (2). The very reason that the heterogeneous material can be homogenized leads us to believe that w_i, w^e and w^m should be asymptotically smaller than the corresponding macroscopic field variables v_i, ψ^e and ψ^m . Substituting equations (15) into (14) and making use of equations (5), we can obtain the leading terms of the functional as

$$\begin{aligned}
 J_1 &= \left\langle \frac{1}{2} \epsilon^{*T} L \epsilon^* + \epsilon^{*T} \eta \theta + \frac{1}{2} c_v \frac{\theta^2}{T_0} \right\rangle + \lambda_i \langle w_i \rangle + \lambda^e \langle w^e \rangle \\
 &+ \lambda^m \langle w^m \rangle + \int_{S_1} \gamma_{i1} \left(w_i^{+1} - w_i^{-1} - \frac{\partial v_i}{\partial x_1} d_1 \right) dS_1 \\
 &+ \int_{S_2} \gamma_{i2} \left(w_i^{+2} - w_i^{-2} - \frac{\partial v_i}{\partial x_2} d_2 \right) dS_2 \\
 &+ \int_{S_3} \gamma_{i3} \left(w_i^{+3} - w_i^{-3} - \frac{\partial v_i}{\partial x_3} d_3 \right) dS_3 \\
 &+ \int_{S_1} \alpha_1 \left(w^{e+1} - w^{e-1} - \frac{\partial \psi^e}{\partial x_1} d_1 \right) dS_1 \\
 &+ \int_{S_2} \alpha_2 \left(w^{e+2} - w^{e-2} - \frac{\partial \psi^e}{\partial x_2} d_2 \right) dS_2 \\
 &+ \int_{S_3} \alpha_3 \left(w^{e+3} - w^{e-3} - \frac{\partial \psi^e}{\partial x_3} d_3 \right) dS_3 \\
 &+ \int_{S_1} \beta_1 \left(w^{m+1} - w^{m-1} - \frac{\partial \psi^m}{\partial x_1} d_1 \right) dS_1
 \end{aligned}$$

$$\begin{aligned}
 & + \int_{S_2} \beta_2 \left(w^{m+2} - w^{m-2} - \frac{\partial \psi^m}{\partial x_2} d_2 \right) dS_2 \\
 & + \int_{S_3} \beta_3 \left(w^{m+3} - w^{m-3} - \frac{\partial \psi^m}{\partial x_3} d_3 \right) dS_3. \quad (17)
 \end{aligned}$$

Here the superscript $+j$ implies evaluate the quantity at $y_j = d_j/2$, and $-j$ implies evaluate the quantity at $y_j = -d_j/2$, for example:

$$\begin{aligned}
 w_i^{+j} &= w_i|_{y_j=d_j/2}, & w_i^{-j} &= w_i|_{y_j=-d_j/2} \\
 & \text{for } j = 1, 2, 3
 \end{aligned}$$

and

$$\epsilon^* = [\epsilon_{11}^* \quad 2\epsilon_{12}^* \quad \epsilon_{22}^* \quad 2\epsilon_{13}^* \quad 2\epsilon_{23}^* \quad \epsilon_{33}^* \\
 E_1^* \quad E_2^* \quad E_3^* \quad H_1^* \quad H_2^* \quad H_3^*]^T \quad (18)$$

along with

$$\begin{aligned}
 \epsilon_{ij}^* &= \frac{1}{2} \left(\frac{\partial w_i}{\partial y_j} + \frac{\partial w_j}{\partial y_i} \right) & E_i^* &= -\frac{\partial w^e}{\partial y_i} \\
 H_i^* &= -\frac{\partial w^m}{\partial y_i}.
 \end{aligned} \quad (19)$$

Although it is possible to carry out the variation of J_1 and find the Euler-Lagrange equations and associated boundary conditions for the unknown functions, which results in inhomogeneous boundary conditions, it is more convenient to use a change of variables to reformulate the same problem so that the boundary conditions are homogeneous. Considering the last nine terms in equation (17), we use the following change of variables as

$$\begin{aligned}
 w_i &= y_j \frac{\partial v_i}{\partial x_j} + \chi_i(\mathbf{x}; \mathbf{y}) & w^e &= y_i \frac{\partial \psi^e}{\partial x_i} + \zeta^e(\mathbf{x}; \mathbf{y}) \\
 w^m &= y_i \frac{\partial \psi^m}{\partial x_i} + \zeta^m(\mathbf{x}; \mathbf{y})
 \end{aligned} \quad (20)$$

where χ_i, ζ^e and ζ^m are the fluctuation functions, satisfying the following constraints in view of equations (2) when the origin of the local coordinate system is chosen to be the center of the UC:

$$\langle \chi_i \rangle = 0 \quad \langle \zeta^e \rangle = 0 \quad \langle \zeta^m \rangle = 0. \quad (21)$$

Substituting equations (20) into (14), we obtain a stationary value problem of a functional defined over the UC for χ_i, ζ^e and ζ^m according to VAM [19], such that

$$\begin{aligned}
 J_\Omega &= \left\langle \frac{1}{2} \epsilon^T L \epsilon + \epsilon^T \eta \theta + \frac{1}{2} c_v \frac{\theta^2}{T_0} \right\rangle + \lambda_i \langle \chi_i \rangle + \lambda^e \langle \zeta^e \rangle \\
 &+ \lambda^m \langle \zeta^m \rangle + \sum_{j=1}^3 \int_{S_j} \gamma_{ij} (\chi_i^{+j} - \chi_i^{-j}) dS_j \\
 &+ \sum_{j=1}^3 \int_{S_j} \alpha_j (\zeta_{+j}^e - \zeta_{-j}^e) dS_j \\
 &+ \sum_{j=1}^3 \int_{S_j} \beta_j (\zeta_{+j}^m - \zeta_{-j}^m) dS_j \quad (22)
 \end{aligned}$$

with

$$\begin{aligned} \chi_i^{+j} &= \chi_i|_{y_j=d_j/2}, & \chi_i^{-j} &= \chi_i|_{y_j=-d_j/2} \\ &\text{for } j = 1, 2, 3 \\ \zeta_{+j}^e &= \zeta^e|_{y_j=d_j/2}, & \zeta_{-j}^e &= \zeta^e|_{y_j=-d_j/2} \\ &\text{for } j = 1, 2, 3 \\ \zeta_{+j}^m &= \zeta^m|_{y_j=d_j/2}, & \zeta_{-j}^m &= \zeta^m|_{y_j=-d_j/2} \\ &\text{for } j = 1, 2, 3. \end{aligned}$$

The matrix ϵ can be expressed as

$$\epsilon = \bar{\epsilon} + \epsilon_1 \quad (23)$$

with

$$\begin{aligned} \bar{\epsilon} &= [\bar{\epsilon}_{11} \quad 2\bar{\epsilon}_{12} \quad \bar{\epsilon}_{22} \quad 2\bar{\epsilon}_{13} \quad 2\bar{\epsilon}_{23} \quad \bar{\epsilon}_{33} \\ &\quad \bar{E}_1 \quad \bar{E}_2 \quad \bar{E}_3 \quad \bar{H}_1 \quad \bar{H}_2 \quad \bar{H}_3]^\text{T} \\ \epsilon_1 &= [\hat{\epsilon}_{11} \quad 2\hat{\epsilon}_{12} \quad \hat{\epsilon}_{22} \quad 2\hat{\epsilon}_{13} \quad 2\hat{\epsilon}_{23} \quad \hat{\epsilon}_{33} \\ &\quad \hat{E}_1 \quad \hat{E}_2 \quad \hat{E}_3 \quad \hat{H}_1 \quad \hat{H}_2 \quad \hat{H}_3]^\text{T} \end{aligned} \quad (24)$$

and

$$\begin{aligned} \bar{\epsilon}_{ij} &= \frac{1}{2} \left(\frac{\partial v_i}{\partial x_j} + \frac{\partial v_j}{\partial x_i} \right) \\ \bar{E}_i &= -\frac{\partial \psi^e}{\partial x_i} & \bar{H}_i &= -\frac{\partial \psi^m}{\partial x_i} \\ \hat{\epsilon}_{ij} &= \frac{1}{2} \left(\frac{\partial \chi_i}{\partial y_j} + \frac{\partial \chi_j}{\partial y_i} \right) \\ \hat{E}_i &= -\frac{\partial \zeta^e}{\partial y_i} & \hat{H}_i &= -\frac{\partial \zeta^m}{\partial y_i} \end{aligned} \quad (25)$$

$\bar{\epsilon}$ will be shown later to be the global multiphysics field variable array containing the strain field, the electric field and the magnetic field for the material with homogenized effective material properties.

The functional J_Ω in equation (22) forms the backbone of the VAMUCH multiphysics micromechanics model. This stationary value of this functional can be solved analytically for very simple cases such as binary composites: however, for general cases we need to use numerical techniques such as the well-developed finite element method (FEM) to seek numerical solutions.

3. Finite element implementation

It is not an efficient way to perform the FEM solution in light of equation (22) because the Lagrange multipliers increase the number of unknowns. In practice, this variational problem can be equivalently formulated as minimizing the following functional:

$$\Pi_\Omega = \frac{1}{\Omega} \int_\Omega \left(\frac{1}{2} \epsilon^\text{T} D \epsilon + \epsilon^\text{T} \eta \theta + \frac{1}{2} c_v \frac{\theta^2}{T_0} \right) d\Omega \quad (26)$$

under the following constraints:

$$\begin{aligned} \chi_i^{+j} &= \chi_i^{-j}, & \zeta_{+j}^e &= \zeta_{-j}^e, & \text{and} \\ \zeta_{+j}^m &= \zeta_{-j}^m & \text{for } j &= 1, 2, 3. \end{aligned} \quad (27)$$

The constraints in equations (21) do not affect the minimum values of Π_Ω but help uniquely determine χ_i , ζ^e and ζ^m . We actually constrain the fluctuation functions at an arbitrary node to be zero and later use this constraint to recover the unique fluctuation functions. The degrees of freedom of the nodes on the positive boundary surface (i.e. $y_i = d_i/2$) are slaved to the nodes on the opposite negative boundary surface (i.e. $y_i = -d_i/2$). By assembling all the independent active degrees of freedom (DOFs), we can implicitly and exactly incorporate the constraints in equations (27).

Introduce the following matrix notation:

$$\epsilon_1 = \begin{bmatrix} \frac{\partial}{\partial y_1} & 0 & 0 & 0 & 0 \\ \frac{\partial}{\partial y_2} & \frac{\partial}{\partial y_1} & 0 & 0 & 0 \\ 0 & \frac{\partial}{\partial y_2} & 0 & 0 & 0 \\ \frac{\partial}{\partial y_3} & 0 & \frac{\partial}{\partial y_1} & 0 & 0 \\ 0 & \frac{\partial}{\partial y_3} & \frac{\partial}{\partial y_2} & 0 & 0 \\ 0 & 0 & \frac{\partial}{\partial y_3} & 0 & 0 \\ 0 & 0 & 0 & -\frac{\partial}{\partial y_1} & 0 \\ 0 & 0 & 0 & -\frac{\partial}{\partial y_2} & 0 \\ 0 & 0 & 0 & -\frac{\partial}{\partial y_3} & 0 \\ 0 & 0 & 0 & 0 & -\frac{\partial}{\partial y_1} \\ 0 & 0 & 0 & 0 & -\frac{\partial}{\partial y_2} \\ 0 & 0 & 0 & 0 & -\frac{\partial}{\partial y_3} \end{bmatrix} \begin{Bmatrix} \chi_1 \\ \chi_2 \\ \chi_3 \\ \zeta^e \\ \zeta^m \end{Bmatrix} \equiv \Gamma_h \chi \quad (28)$$

where Γ_h is an operator matrix. The multiphysics fluctuation vector χ can be discretized using finite elements as

$$\chi(x_i; y_i) = S(y_i) \mathcal{X}(x_i) \quad (29)$$

with S representing the shape functions and \mathcal{X} a column matrix of the nodal values of the mechanical, electric and magnetic fluctuation functions. Substituting equations (28) and (29) into equation (26), the discretized version of the functional is obtained as

$$\begin{aligned} \Pi_\Omega &= \frac{1}{2\Omega} \left(\mathcal{X}^\text{T} E \mathcal{X} + 2\mathcal{X}^\text{T} D_{h\epsilon} \bar{\epsilon} + \bar{\epsilon}^\text{T} D_{\epsilon\epsilon} \bar{\epsilon} \right. \\ &\quad \left. + 2\mathcal{X}^\text{T} D_{h\theta} \theta + 2\bar{\epsilon}^\text{T} D_{\epsilon\theta} \theta + D_{\theta\theta} \frac{\theta^2}{T_0} \right) \end{aligned} \quad (30)$$

where

$$\begin{aligned} E &= \int_\Omega (\Gamma_h S)^\text{T} D (\Gamma_h S) d\Omega & D_{h\epsilon} &= \int_\Omega (\Gamma_h S)^\text{T} D d\Omega \\ D_{\epsilon\epsilon} &= \int_\Omega D d\Omega & D_{h\theta} &= \int_\Omega (\Gamma_h S)^\text{T} \eta d\Omega \\ D_{\epsilon\theta} &= \int_\Omega \eta d\Omega & D_{\theta\theta} &= \int_\Omega c_v d\Omega. \end{aligned}$$

Minimizing Π_Ω in equation (30), we obtain the following linear system:

$$E \mathcal{X} = -D_{h\epsilon} \bar{\epsilon} - D_{h\theta} \theta. \quad (31)$$

The fluctuation function \mathcal{X} in equation (31) is linearly proportional to $\bar{\epsilon}$ and θ so that the solution can be written symbolically as

$$\mathcal{X} = \mathcal{X}_0 \bar{\epsilon} + \mathcal{X}_\theta \theta. \quad (32)$$

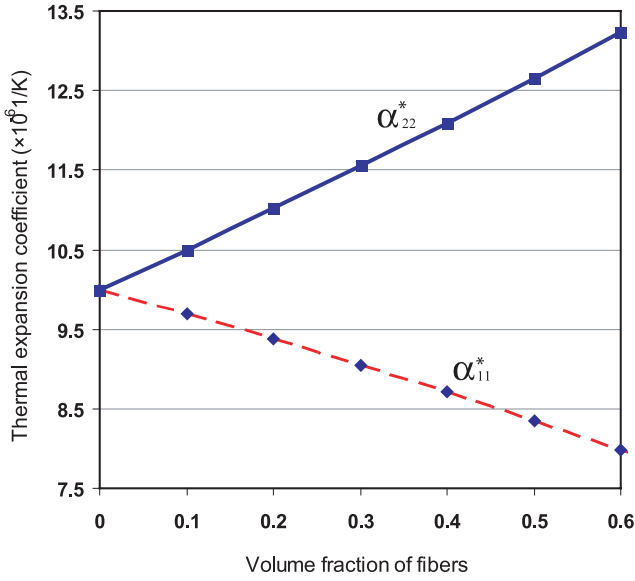


Figure 2. Effective thermal expansion coefficients α_{11}^* and α_{33}^* .

Table 1. Material properties of the composite constituents (BaTiO₃, CoFe₂O₄ and epoxy).

	BaTiO ₃	CoFe ₂ O ₄	Epoxy
C_{11} (GPa)	162	269.5	5.53
C_{12} (GPa)	78	170	2.97
C_{23} (GPa)	77	173	2.97
C_{22} (GPa)	166	286	5.53
C_{55} (GPa)	43	45.3	1.28
k_{11} ($\times 10^{-9}$ C V ⁻¹ m ⁻¹)	12.6	0.093	0.1
k_{33} ($\times 10^{-9}$ C V ⁻¹ m ⁻¹)	11.2	0.08	0.1
μ_{11} ($\times 10^{-4}$ N s ² C ⁻²)	0.1	1.57	0.01
μ_{33} ($\times 10^{-4}$ N s ² C ⁻²)	0.05	-5.9	0.01
e_{11} (C m ⁻²)	18.6	0	0
e_{21} (C m ⁻²)	-4.4	0	0
e_{51} (C m ⁻²)	11.6	0	0
q_{11} (N A ⁻¹ m ⁻¹)	0	699.7	0
q_{21} (N A ⁻¹ m ⁻¹)	0	580.3	0
q_{51} (N A ⁻¹ m ⁻¹)	0	550	0
α_{11} ($\times 10^{-6}$ K ⁻¹)	6.4	10	54
α_{22} ($\times 10^{-6}$ K ⁻¹)	15.7	10	54
α_{33} ($\times 10^{-6}$ K ⁻¹)	15.7	10	54
c_v (kJ m ⁻³ K ⁻¹)	3193.62	2000	—

Substituting equation (32) into (30), we obtain the thermodynamic potential density of the UC as

$$\Pi_{\Omega} = \frac{1}{2} \bar{\epsilon}^T \bar{D} \bar{\epsilon} + \bar{\epsilon}^T \bar{\eta} \theta + \frac{1}{2} c_v^* \frac{\theta^2}{T_0} \quad (33)$$

with

$$\begin{aligned} \bar{D} &= \frac{1}{\Omega} (\mathcal{X}_0^T D_{h\epsilon} + D_{\epsilon\epsilon}) \\ \bar{\eta} &= \frac{1}{\Omega} \left[\frac{1}{2} (D_{h\epsilon}^T \mathcal{X}_\theta + \mathcal{X}_0^T D_{h\theta}) + D_{\epsilon\theta} \right] \\ \bar{c}_v &= \frac{1}{\Omega} [\mathcal{X}_\theta^T D_{h\theta} T_0 + D_{\theta\theta}] \end{aligned}$$

where $\bar{\epsilon}$ is a column matrix containing the global strains, global electric fields and global magnetic fields; \bar{D} in equation (33)

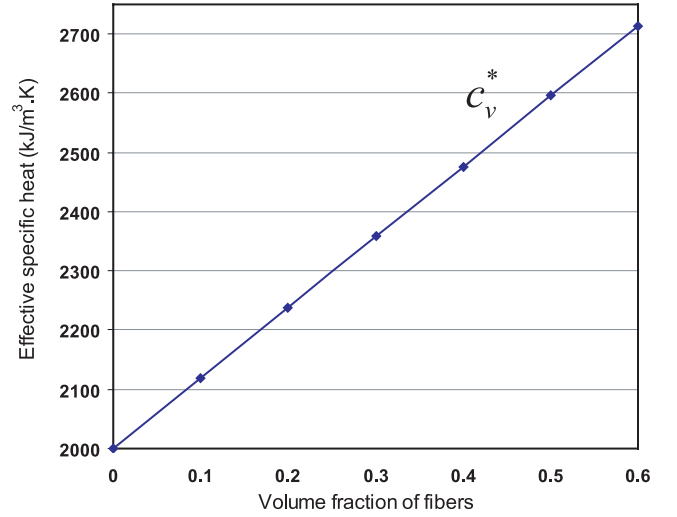


Figure 3. Effective specific heat c_v^* .

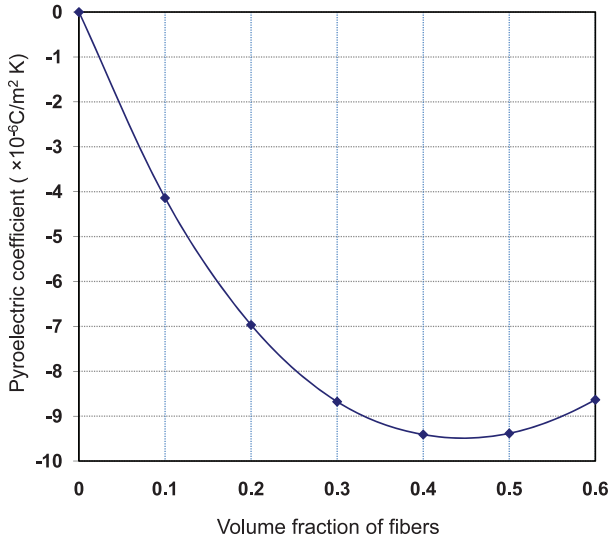
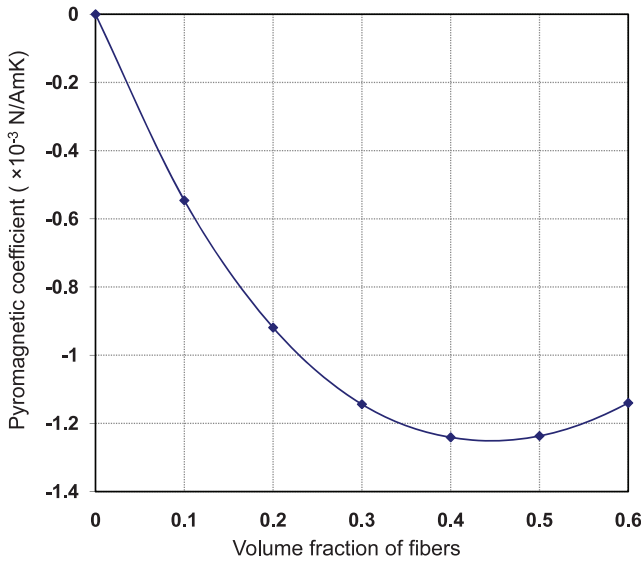
is a 12×12 effective material matrix containing the effective multiphysics material properties which can be expressed as

$$\bar{D} = \begin{bmatrix} C^* & -e^* & -q^* \\ -e^{*T} & -k^* & -a^* \\ -q^{*T} & -a^{*T} & -\mu^* \end{bmatrix} \quad (34)$$

$\bar{\eta}$ is a 12×1 effective matrix containing the effective second-order thermal stress tensor Λ_{ij}^* , the effective pyroelectric vector p_i^* and the effective pyromagnetic vector m_i^* ; \bar{c}_v is the effective specific heat. Note that the effective coefficients of thermal expansion (CTEs) can be calculated as

$$\alpha_{ij}^* = -(C_{ijkl}^*)^{-1} \Lambda_{kl}^*. \quad (35)$$

Having obtained the effective multiphysics properties, we can use these properties to carry out the macroscopic analysis of the complete structure to predict the global multiphysics behavior of the engineering system made of smart materials. Sometimes, we also need the pointwise distribution of the multiphysical fields within the microstructure. To this end, we can carry out a recovery procedure based on the fluctuation functions χ we have obtained in the micromechanical analysis and the global behavior we predicted from the macroscopic analysis. Specifically, we can recover the local fields, such as local displacements, electric potential, magnetic potential, stresses, electric displacements and magnetic flux density in terms of the macroscopic behavior including the global displacements v_i , the global electric potential ψ^e , the global magnetic potential ϕ^m , the temperature variation θ and the global field variables contained in $\bar{\epsilon}$. First, the fluctuation functions should be uniquely determined using the constraints in equations (21). Then, we can recover the local displacements, electric potential and magnetic potential using equations (15) and (20) as


 Figure 4. Effective pyroelectric constant p_1^* .

 Figure 5. Effective pyromagnetic constant m_1^* .

$$\begin{Bmatrix} u_1 \\ u_2 \\ u_3 \\ \phi^e \\ \phi^m \end{Bmatrix} = \begin{Bmatrix} v_1 \\ v_2 \\ v_3 \\ \psi^e \\ \psi^m \end{Bmatrix} + \begin{bmatrix} \frac{\partial v_1}{\partial x_1} & \frac{\partial v_1}{\partial x_2} & \frac{\partial v_1}{\partial x_3} \\ \frac{\partial v_2}{\partial x_1} & \frac{\partial v_2}{\partial x_2} & \frac{\partial v_2}{\partial x_3} \\ \frac{\partial v_3}{\partial x_1} & \frac{\partial v_3}{\partial x_2} & \frac{\partial v_3}{\partial x_3} \\ \frac{\partial \psi^e}{\partial x_1} & \frac{\partial \psi^e}{\partial x_2} & \frac{\partial \psi^e}{\partial x_3} \\ \frac{\partial \psi^m}{\partial x_1} & \frac{\partial \psi^m}{\partial x_2} & \frac{\partial \psi^m}{\partial x_3} \end{bmatrix} \begin{Bmatrix} y_1 \\ y_2 \\ y_3 \end{Bmatrix} + \bar{S}\bar{\mathcal{X}}. \quad (36)$$

Here \bar{S} is different from S due to the recovery of slave nodes and the constrained node. The local strain field, the electric field and the magnetic field can be recovered using equation (23) along with equation (28) as

$$\epsilon = \bar{\epsilon} + \Gamma_h \bar{S}\bar{\mathcal{X}}. \quad (37)$$

The local stress, the electric displacement field and the magnetic flux density can be recovered straightforwardly using the 3D constitutive relations for the constituent material as

$$\sigma = L\epsilon + \eta\theta \quad (38)$$

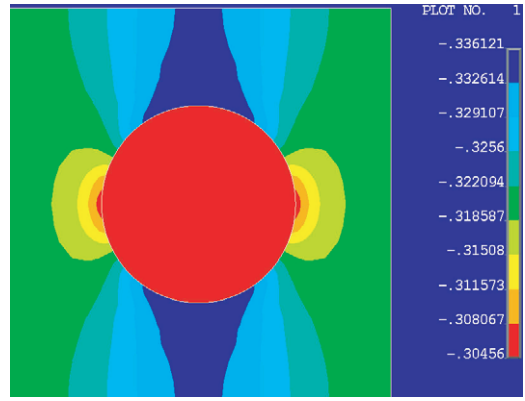
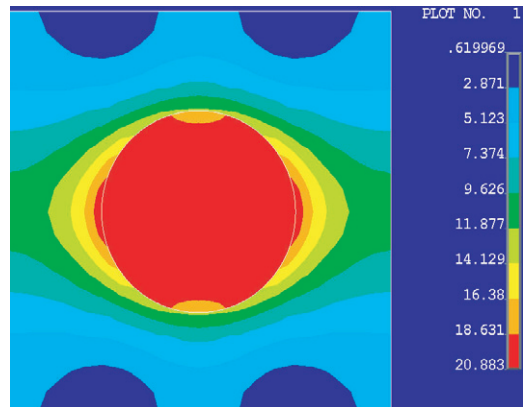

 Figure 6. Contour plot of σ_{22} (GPa).


Figure 7. Contour plot of von Mises stress (GPa).

where σ is a column matrix containing 3D stresses, electric displacements and magnetic flux density such that

$$\sigma = \begin{bmatrix} \sigma_{11} & \sigma_{12} & \sigma_{22} & \sigma_{13} & \sigma_{23} & \sigma_{33} \\ -D_1 & -D_2 & -D_3 & -B_1 & -B_2 & -B_3 \end{bmatrix}^T \quad (39)$$

where σ_{ij} , D_i and B_i denote the stress tensor, the electric flux density vector and the magnetic flux density vector, respectively.

Although VAMUCH is implemented using the finite element technique, it is not one of the finite-element-analysis (FEA)-based micromechanics approaches and it is dramatically different from FEA-based approaches, both in its theory and its application, as pointed out in [21]. Nevertheless, VAMUCH takes full advantage of the finite element technique as far as efficiency and convenience concerned including the versatile discretization capability for arbitrary microstructure, a highly efficient linear solver, well-developed preprocessing and postprocessing capabilities.

4. Numerical results

The predictive capability of the effective properties of VAMUCH has been demonstrated using many examples [14]. In this section, we will use VAMUCH to predict the effective elastic, piezoelectric, piezomagnetic, dielectric and magnetic permeability, and electromagnetic coupling constants as well

Table 2. Material properties of PZT-5 and polymer.

	C_{11} (GPa)	C_{12} (GPa)	C_{23} (GPa)	C_{22} (GPa)	C_{44} (GPa)	C_{66} (GPa)
PZT-5	111	75.2	75.4	121	22.8	21.1
Polymer	3.86	2.57	2.57	3.86	0.64	0.64
	e_{11}	e_{21}	e_{51}	k_{11}	k_{33}	
PZT-5	15.8	-5.4	12.3	7.35	8.11	
Polymer	0	0	0	0.079 65	0.079 65	

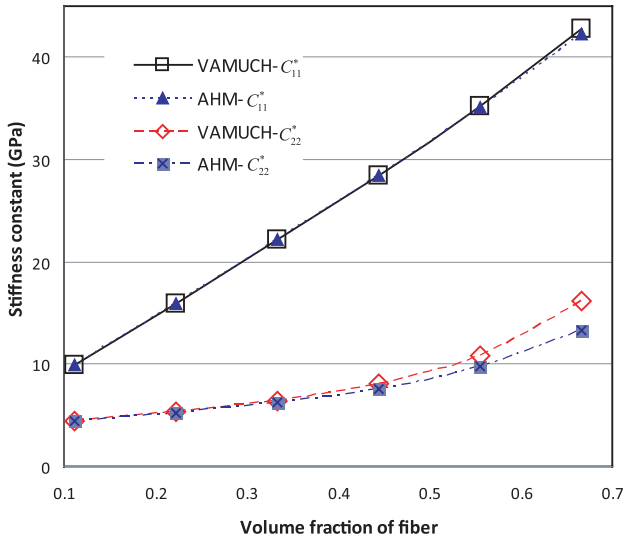


Figure 8. Effective stiffness constants C_{11}^* and C_{22}^* .

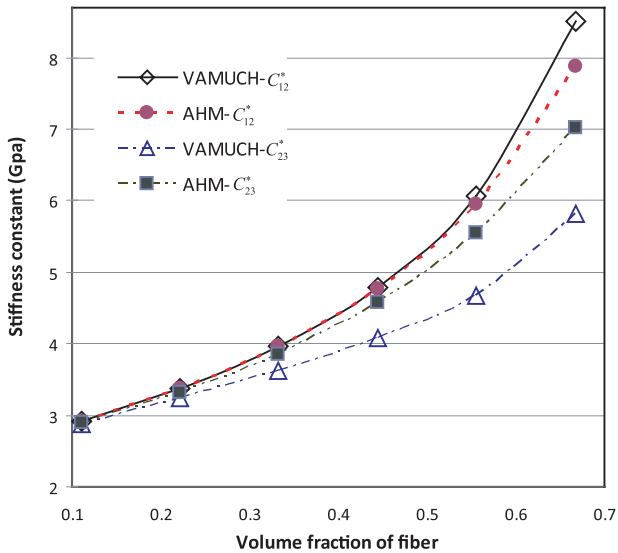


Figure 9. Effective stiffness constants C_{12}^* and C_{23}^* .

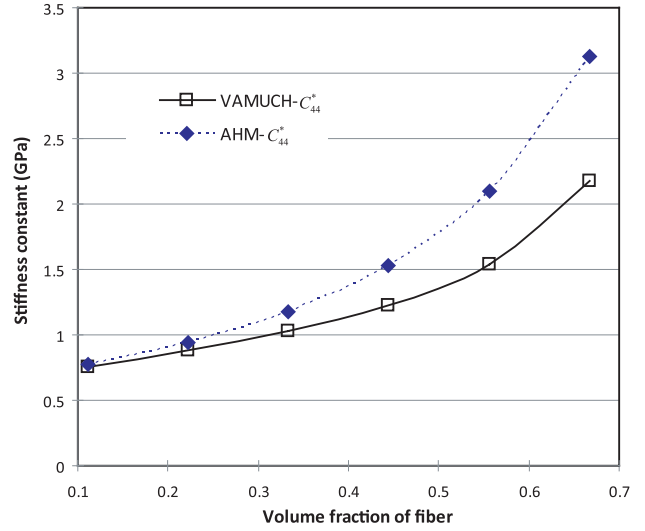


Figure 10. Effective stiffness constant C_{44}^* .

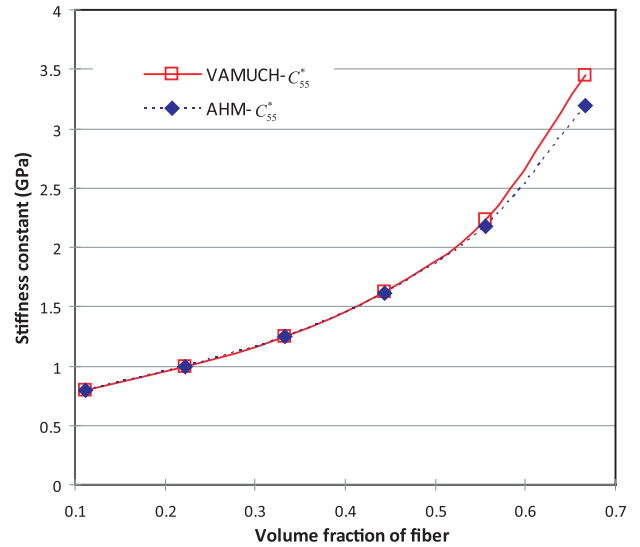


Figure 11. Effective stiffness constant C_{55}^* .

as the coefficients of thermal expansion, pyroelectric and pyromagnetic coefficients, and specific heat and recover the distribution of the local fields.

4.1. Two-phase composites

In this section, the first example is a two-phase composite composed of a CoFe_2O_4 piezomagnetic matrix reinforced by BaTiO_3 piezoelectric fibers which is an example extensively investigated in [6, 9, 10]. The piezoelectric fibers are of circular shape and arranged in a square array. Both constituents are

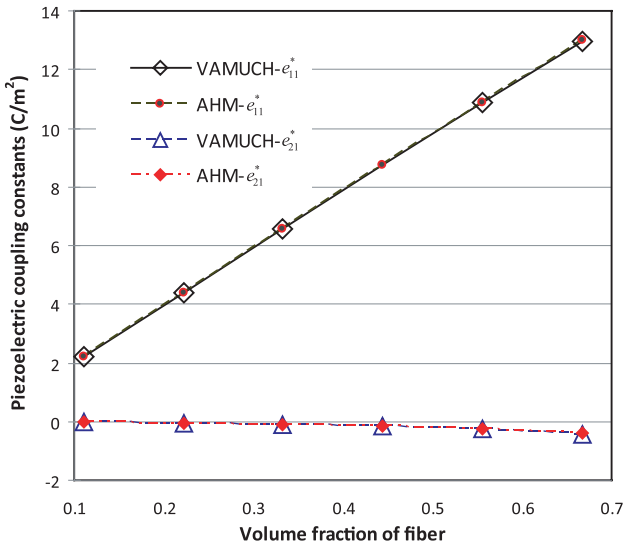


Figure 12. Effective piezoelectric coupling constants e_{11}^* and e_{21}^* .

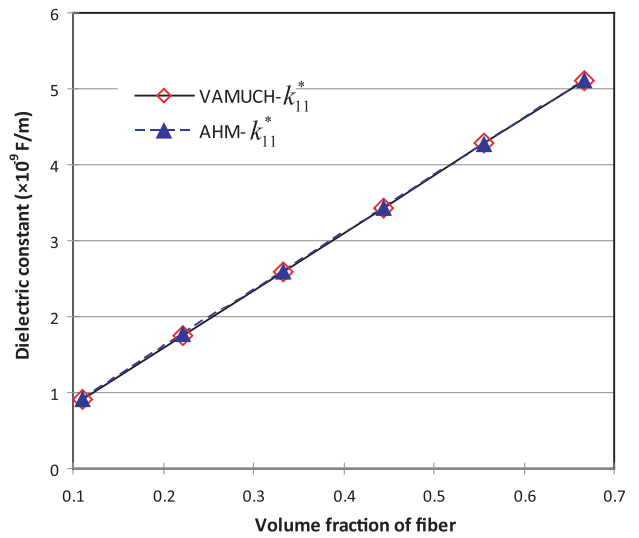


Figure 14. Effective dielectric constant k_{11}^* .

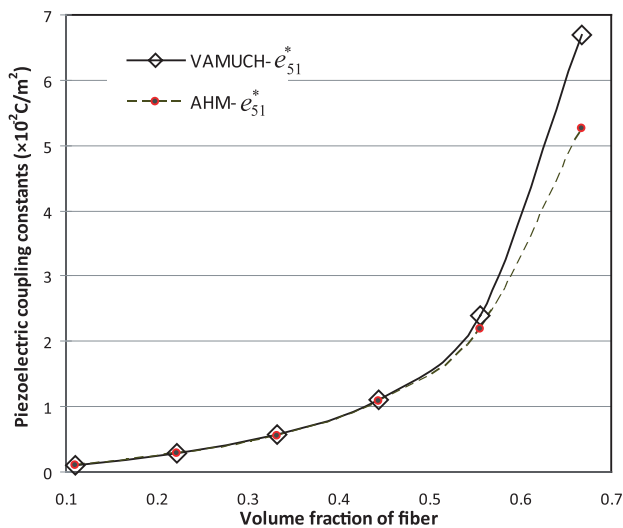


Figure 13. Effective piezoelectric coupling constant e_{51}^* .

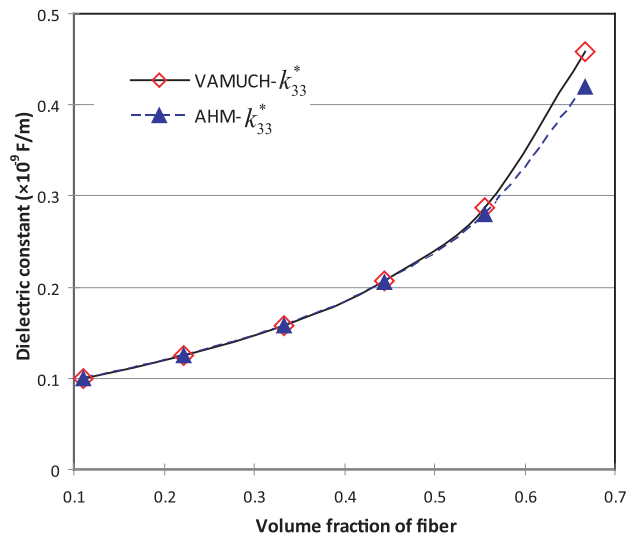


Figure 15. Effective dielectric constant k_{33}^* .

transversely isotropic with the axis of symmetry oriented in the 1 direction. The material properties of constituents are given in table 1, which are taken from [6].

Figures 2 and 3 show the effective coefficients of thermal expansion (CTEs) and specific heat varying with the volume fraction of BaTiO₃. It can be observed that the effective transverse CTE α_{22}^* and specific heat increase linearly with respect to the volume fraction of fibers while the effective axial CTE α_{11}^* decreases linearly with respect to the volume fraction of fibers. The effective pyroelectric and pyromagnetic constants of the composite are illustrated in figures 4 and figure 5, respectively, although they are absent in either of the individual phases. It can be observed that these two effective properties vary quadratically with respect to the volume fraction of fibers and reach the minimum when the volume fraction of the fiber is about 50%.

VAMUCH can also accurately recover the local distribution of the field variables based on the macroscopic be-

havior. Figures 6 and 7 show the contour plots of the distributions of σ_{22} and von Mises stress within the UC with a volume fraction of fiber (VOF) 20% induced by a macroscopic normal strain $\bar{\epsilon}_{22} = 0.1\%$, macroscopic electric field $\bar{E}_2 = 100 \text{ V m}^{-1}$ and 100 K uniform temperature arising from a stress-free state. It is pointed out that it is very difficult, if not impossible, to predict the local fields corresponding to a macroscopic state with combined macroscopic field variables using a finite-element-analysis-based micromechanics approach because different field variables require different sets of boundary conditions, while VAMUCH has no such difficulty and one can simultaneously prescribe all the field variables including mechanical displacements, electric potential, magnetic potential, strain field, electric field, magnetic field and temperature field because no boundary conditions on the macroscopic field variables are needed.

The second example is a piezoelectric fiber-reinforced polymer matrix composite which is extensively investigated

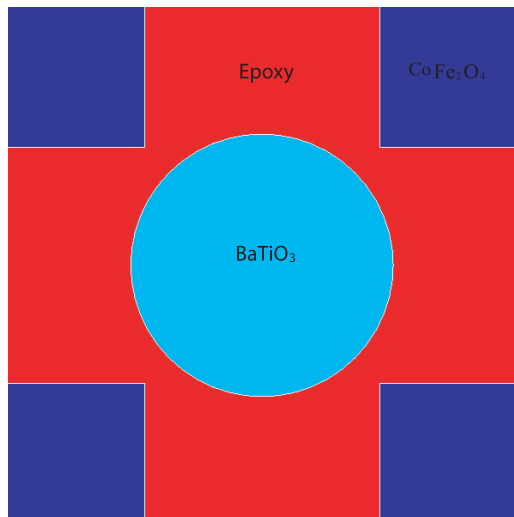


Figure 16. Unit cell of a three-phase composite.

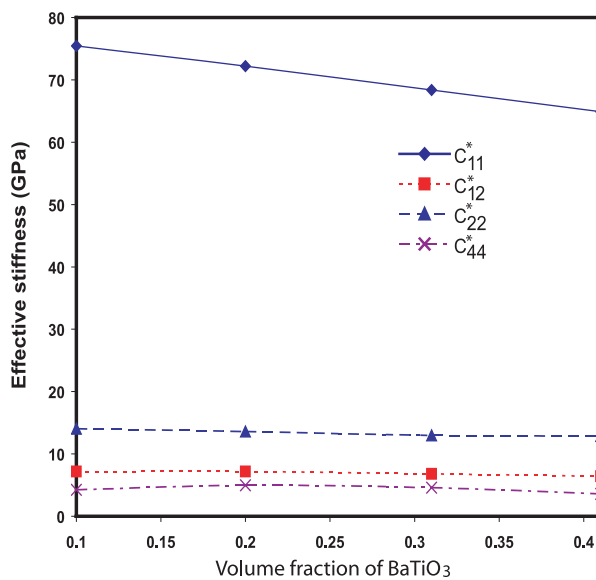


Figure 17. Effective stiffness coefficients.

in [22, 23]. The cylindrical PZT-5 fibers are distributed in a square array in a polymer matrix. The material properties of both components are shown in table 2, which are taken from [23]. The units of these properties are: elastic constants (GPa), piezoelectric constants (C m^{-2}) and dielectric constants (10^{-9} F m^{-1}). The effective properties of the composites predicted by VAMUCH are compared with those calculated by the two-scale asymptotic homogenization method (AHM) [16, 24, 25] and finite element analysis. A brief description of the finite element analysis and AHM are given in [22]. All effective coefficients are calculated for six different volume fractions of fibers (0.111, 0.222, 0.333, 0.444, 0.556 and 0.667). We found out that the results of VAMUCH are almost the same as those of finite element analysis in [23] so that we only plot the variation of effective properties with the volume fraction of fibers computed by VAMUCH and AHM in figures 8–15. It can be seen that the

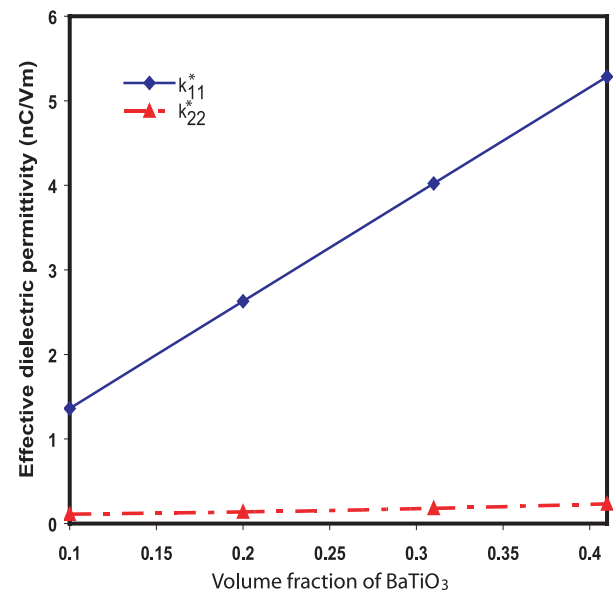


Figure 18. Effective dielectric permittivity.

results of both approaches have excellent agreement for most of the effective properties, except the prediction of C_{44}^* and C_{23}^* having significant differences at high volume fraction of fibers. As pointed out in [23], this is mainly due to the assumed transverse isotropy on which the analytical solution of AHM is based. It is noted that the AHM results are directly taken from the tabulated data in [22].

4.2. Three-phase composites

The three-phase electro-magneto-elastic composite considered consists of an elastic epoxy matrix reinforced with piezoelectric (BaTiO_3) and piezomagnetic fibers (CoFe_2O_4). The piezoelectric fiber is of circular shape and at the center of the unit cell while the piezomagnetic fibers in the shape of quarter squares are located at the four corners of the UC as shown in figure 16. The material properties of the three constituents are listed in table 1. Figures 17–26 show the variation of the effective properties of composites with respect to the volume fractions of the piezoelectric fibers (BaTiO_3) when the matrix volume fraction is fixed at 0.5.

As one can observe from figure 17, the effective stiffness coefficient C_{11}^* decreases slightly with respect to the volume fraction of piezoelectric fibers while other stiffness coefficients including C_{12}^* , C_{22}^* and C_{44}^* remain almost the same. One reason is that the elastic moduli of piezoelectric fibers are similar to those of piezomagnetic fibers and the total volume fraction of these two fibers remains fixed.

As one can observe from figure 18, the effective axial dielectric permittivity k_{11}^* increases significantly with respect to the volume fraction of piezoelectric fibers while the effective transverse dielectric permittivity k_{22}^* remains almost invariant with respect to the change of the volume fraction of piezoelectric fibers. A similar trend is found in effective piezoelectric coefficients, as shown in figure 19. It seems only e_{11}^* is significant and the other piezoelectric coefficients are almost negligible.

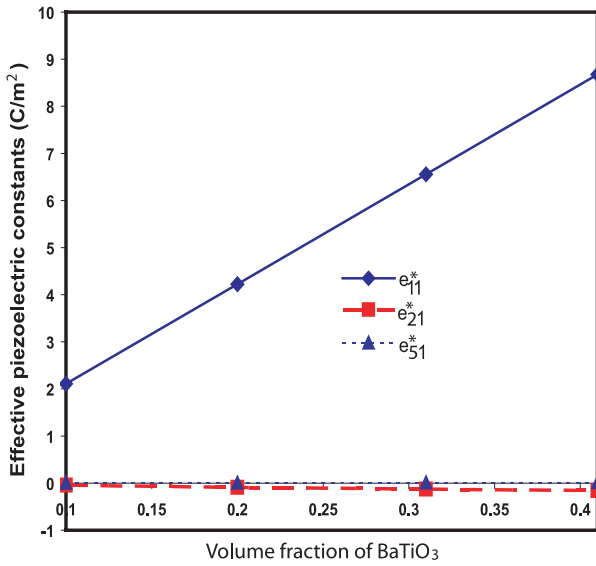


Figure 19. Effective piezoelectric constants.

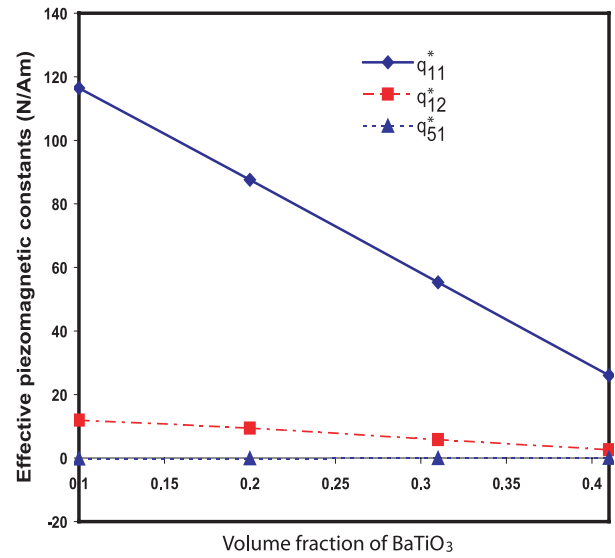


Figure 21. Effective piezomagnetic constants.

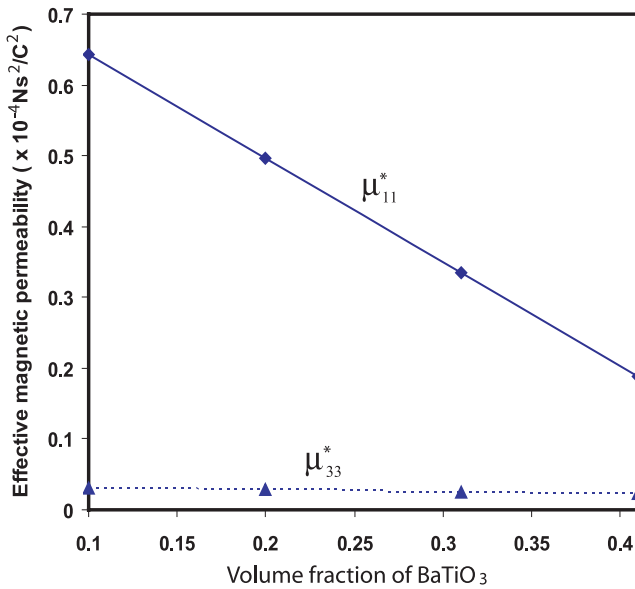


Figure 20. Effective magnetic permeability.

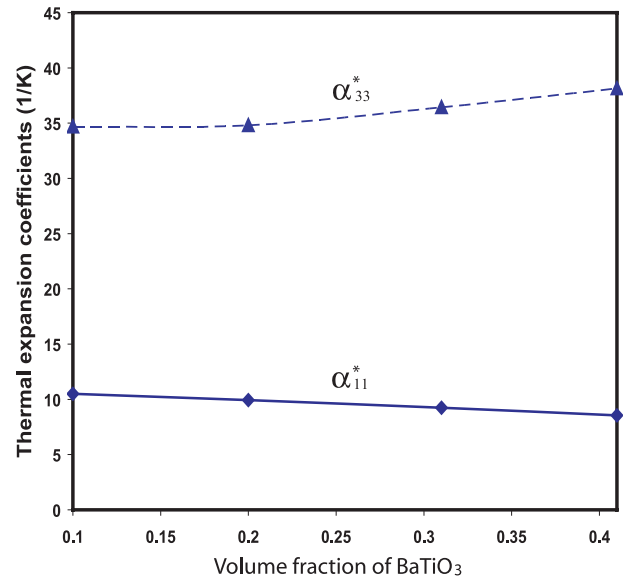


Figure 22. Effective CTEs.

As one can observe from figure 20, the effective axial magnetic permeability μ_{11}^* decreases significantly with respect to the volume fraction of piezoelectric fibers while the effective transverse magnetic permeability μ_{33}^* remains almost invariant with respect to the change of the volume fraction of piezoelectric fibers. A similar trend is found in effective piezomagnetic coefficients, as shown in figure 21. However, except that q_{11}^* decreases with respect to the volume fraction of piezoelectric fibers, q_{12}^* also decreases slightly and q_{51}^* is negligible.

Figure 22 shows the distribution of the effective CTEs. One can observe that the effective transverse CTE α_{33}^* is almost three times the axial CTE α_{11}^* although both of them only change slightly with respect to the volume fraction of the piezoelectric fibers.

We also find out that this composite has some new material properties which are not available in any of its constituents but are generated due to the interplay of different phases. For example, this composite has significant electromagnetic coupling along both the axial direction and the transverse direction. The maximum electromagnetic coupling is generated when the volume fraction is around 25%, as shown in figures 23 and 24. Some new couplings between the thermal field and the electromagnetic field represented by pyroelectric coefficients and pyromagnetic coefficients are also generated as shown in figures 25 and 26.

5. Conclusion

The variational asymptotic method has been used to construct a fully coupled micromechanics model for prediction of

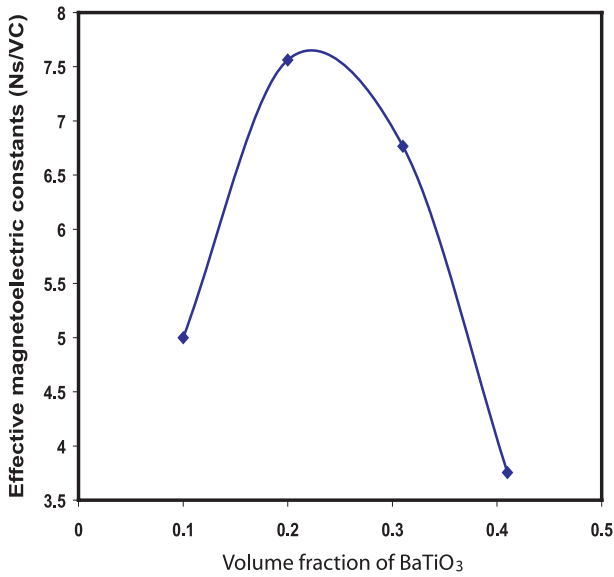


Figure 23. Effective electromagnetic constants a_{11}^* .

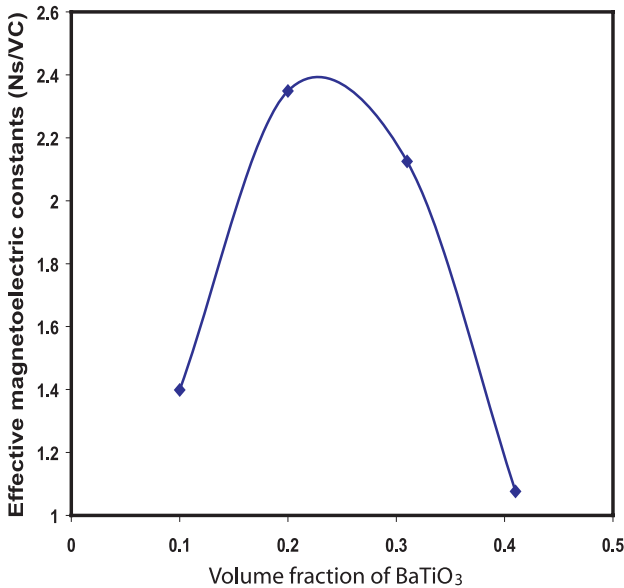


Figure 24. Effective electromagnetic constants a_{33}^* .

effective properties of smart composites which could be responsive to thermal, electric, magnetic and mechanical fields. This multiphysics micromechanics model not only predicts the complete set of effective multiphysics properties but also accurately recovers the distribution of the local fields. Its theoretical derivation invokes two basic assumptions associated with the micromechanics concept. It has been implemented in the computer program VAMUCH using the finite element technique so that it can model microstructures with any number of phases with arbitrary geometry. It provides a versatile tool for the design and analysis of smart composite materials to engineer the microstructure for desirable material properties.

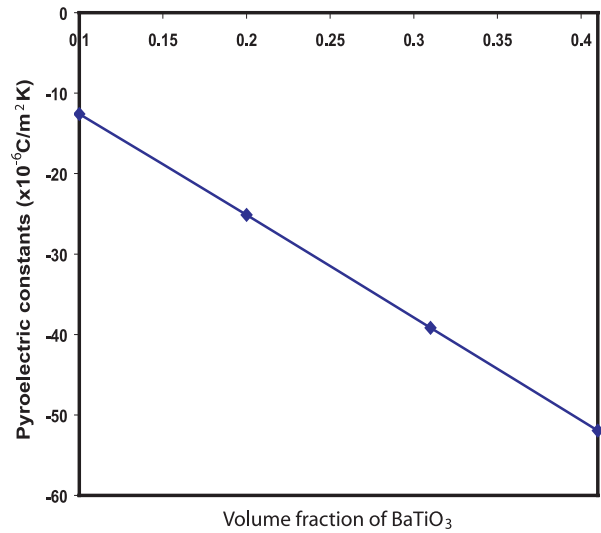


Figure 25. Effective pyroelectric coefficients p_1^* .

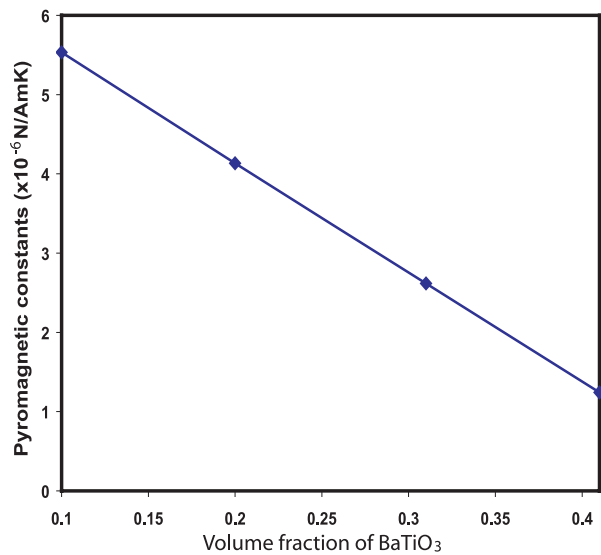


Figure 26. Effective pyromagnetic coefficients m_1^* .

Acknowledgments

This work is supported, in part, by the National Science Foundation under grant DMI-0522908 and the State of Utah Community/University Research Initiative Grant. The views and conclusions contained herein are those of the authors and should not be interpreted as necessarily representing the official policies or endorsement, either expressed or implied, of the funding agencies.

References

- [1] Nan C W 1994 Magnetolectric effect in composites of piezoelectric and piezomagnetic phases *Phys. Rev. B* **50** 6082–8
- [2] Lagoudas D C, Boyd J G and Bo Z 1994 Micromechanics of active composites with sma fibers *J. Eng. Mater. Technol.* **116** 337–45

- [3] Ekimov E A *et al* 2002 Mechanical behavior and microstructure of nanodiamond-based composite materials *J. Mater. Sci. Lett.* **21** 1699–702
- [4] Shen L and Li J 2005 Homogenization of a fiber/sphere with an inhomogeneous interphase for the effective elastic moduli of composites *Proc. R. Soc. A* **461** 1475–504
- [5] Sevostianov I and Kachanov M 2006 Homogenization of a nanoparticle with graded interphase *Int. J. Fract.* **139** 121–7
- [6] Li J Y and Dunn M L 1998 Micromechanics of magneto-electroelastic composite materials: average fields and effective behavior *J. Intell. Mater. Syst. Struct.* **9** 404–16
- [7] Mori T and Tanaka K 1973 Average stress in matrix and average elastic energy of materials with misfitting inclusions *Acta Metall.* **21** 571–4
- [8] Aboudi J 2001 Micromechanical analysis of fully coupled electro-magneto-thermo-elastic multiphase composites *Smart Mater. Struct.* **10** 867–77
- [9] Lee J S, Boyd J G and Lagoudas D C 2005 Effective properties of three-phase electro-magneto-elastic composites *Int. J. Eng. Sci.* **43** 790–825
- [10] Tang T and Yu W 2008 Variational asymptotic homogenization of heterogeneous electromagnetoelastic materials *Int. J. Eng. Sci.* **46** 741–57
- [11] Yu W and Tang T 2007 Variational asymptotic method for unit cell homogenization of periodically heterogeneous materials *Int. J. Solids Struct.* **44** 3738–55
- [12] Yu W and Tang T 2007 A variational asymptotic micromechanics model for predicting thermoelastic properties of heterogeneous materials *Int. J. Solids Struct.* **44** 7510–25
- [13] Tang T and Yu W 2007 A variational asymptotic micromechanics model for predicting conductivity of composite materials *J. Mech. Mater. Struct.* **2** 1813–30
- [14] Tang T and Yu W 2008 Variational asymptotic micromechanics modeling of heterogeneous piezoelectric materials *Mech. Mater.* **40** 812–24
- [15] Berdichevsky V L 1979 Variational-asymptotic method of constructing a theory of shells *Prikl. Mat. Mekh.* **43** 664–87
- [16] Bensoussan A, Lions J L and Papanicolaou G 1978 *Asymptotic Analysis for Periodic Structures* (Amsterdam: North-Holland)
- [17] Guedes J M and Kikuchi N 1990 Preprocessing and postprocessing for materials based on the homogenization method with adaptive finite element method *Comput. Methods Appl. Mech. Eng.* **83** 143–98
- [18] Kalamkarov A L and Kolpakov A G 1997 *Analysis, Design and Optimization of Composite Structures* vol 1 and 2 (New York: Wiley)
- [19] Berdichevsky V L 1977 On averaging of periodic systems *Prikl. Mat. Mekh.* **41** 993–1006
- [20] Kunin I 1982 *Theory of Elastic Media with Microstructure* vol 1 and 2 (Berlin: Springer)
- [21] Tang T 2008 Variational asymptotic micromechanics modeling of composite materials *PhD Thesis* Mechanical and Aerospace Engineering, Utah State University August 2008
- [22] Berger H, Gabbert U, Köppe R R, Bravo-Castillero J, Guinovart-Diaz R, Otero J A and Maugin G A 2003 Finite element and asymptotic homogenization methods applied to smart composite materials *Comput. Mech.* **33** 61–7
- [23] Berger H, Kari S, Gabbert U, Rodriguez-Ramos R, Guinovart-Diaz R, Otero J A and Bravo-Castillero J 2005 An analytical and numerical approach for calculating effective material coefficients of piezoelectric fiber composites *Int. J. Solids Struct.* **42** 5692–714
- [24] Guinovart-Diaz R, Bravo-Castillero J, Rodriguez-Ramos R and Sabina F J 2001 Closed-form expressions for the effective coefficients of a fiber-reinforced composite with transversely isotropic constituents i. elastic and hexagonal symmetry *J. Mech. Phys. Solids* **49** 1445–62
- [25] Sabina F J, Rodriguez-Ramos R, Bravo-Castillero R and Guinovart-Diaz J 2001 Closed-form expressions for the effective coefficients of a fiber-reinforced composite with transversely isotropic constituents i. piezoelectric and hexagonal symmetry *J. Mech. Phys. Solids* **49** 1463–79